Tritium burn efficiency in deuterium-tritium magnetic fusion

Tritium burn efficiency in deuterium–tritium magnetic fusion

OPEN ACCESS
IOP Publishing | International Atomic Energy Agency
Nuclear Fusion
Nucl. Fusion 63 (2023) 126019 (10pp)
https://doi.org/10.1088/1741-4326/acf3fb

Tritium burn efficiency in deuterium–tritium magnetic fusion

D.G. Whyte[1], R. Delaporte-Mathurin[1], S.E. Ferry[1,*] and S. Meschini[2]

[1] Plasma Science and Fusion Center, Massachusetts Institute of Technology, Cambridge, MA 02139, United States of America
[2] Politecnico di Torino, Corso Duca degli Abruzzi 24, Torino 10129, Italy

E-mail: seferry@mit.edu

Received 13 June 2023, revised 9 August 2023
Accepted for publication 25 August 2023
Published 25 September 2023

CrossMark

Abstract
The controlling parameters regarding tritium burn efficiency (TBE) are derived from first principles and shown to depend fundamentally on the permitted He gas fraction in the divertor and effective pumping speeds of He ash and unburned hydrogenic fuel. The analysis is generic to any equilibrated magnet fusion plasma using a divertor for particle exhaust. The He gas fraction in the plasma limits the maximum TBE due to the link between ash dilution effects in the core plasma and fusion performance. High TBE in magnetic fusion devices is counter-correlated to achieving high gain and power density for commercial fusion. The impact of TBE on fusion performance for several figures of merit are derived, including power density, required $n - \tau_e$ product, and plasma energy gain Q_p. The TBE formulation presented here is applied to existing devices, based on published data of enrichment and τ^*_He from research tokamaks. This assessment strongly motivates exploration of technologies that would enhance the effective pumping speed of He to fuel out of the plasma.

Keywords: tritium, fuel cycle, divertor, helium ash

(Some figures may appear in colour only in the online journal)

1. Introduction

The topic of tritium self-sufficiency in fusion power plants (FPPs) is gaining more attention in academic studies [1] and in the popular science press [2] with the growth of the commercial fusion energy sector. It is expected that the first commercial FPPs will utilize the deuterium–tritium (D–T) fusion cycle. D–T fusion has well-known advantages over other fusion fuels, including a ∼100× higher reactivity at experimentally achieved plasma temperatures (∼10–20 keV), and access to ignition and high gain (Q_p) at lower T and lower $n\tau_E$ product [3] due to its high reactivity and significant energy release per reaction (17.6 MeV). The D–T reaction creates two particles: a helium ion (or alpha, α) and a free neutron (n). Unlike deuterium, which is stable and highly abundant, natural tritium reserves are effectively non-existent. Tritium made from neutron capture in heavy-water moderated fission plants has very limited reserves (∼35 kg worldwide [4]) which is insufficient to supply fuel to a D–T fusion power industry. This necessitates that D–T FPPs produce their own tritium via (n,t) capture reactions with lithium isotopes in the breeding blanket that surrounds the plasma core. Deuterium and lithium are thus the consumables in D–T fusion. Tritium, and its additional neutron as compared to deuterium, is continuously

[*] Author to whom any correspondence should be addressed.

recycled and can be considered as a catalyst that improves the fusion performance in the FPP. Therefore, FPP designs must assure tritium self-sufficiency, which is a multi-faceted design requirement referring to an FPP's ability (1) to breed and recover sufficient tritium for its own fueling needs, (2) secure sufficient tritium reserves to assure continued operation and (3) provide the startup inventory for additional FPPs. The FPP's tritium supply strategy must consider the effectiveness of tritium fuel consumption (the subject matter of this work), the rates at which tritium is bred in the blanket, the characteristic timescales required to recover and process bred and recycled tritium, and the on-site reserve tritium inventory that is required.

This work develops and quantifies a dimensionless figure of merit, **tritium burn efficiency** (TBE), which describes the global effectiveness of tritium in an FPP that creates fusion power with a confined plasma equilibrated on a long timescale. We argue that TBE tends to apply to most magnetic FPP concepts and should be used when characterizing the fuel cycle of these systems. The TBE metric provides conceptual clarity on tritium use efficiency in magnetic confinement fusion (MCF) devices, which utilize continuous fueling systems that are controlled by different processes than do FPP concepts in which fuel is introduced and burned in discrete events, such as inertial confinement fusion (ICF) or magneto-inertial fusion (MIF).

In systems featuring discrete fusion events, like ICF and MIF, it is conceptually appropriate to use burn fraction f_b and fueling efficiency η_f to characterize the fuel cycle instead of TBE. f_b is defined as the fraction of fuel burned in the plasma in a single compression or ignition event, while η_f describes the maximum percentage of tritium fuel introduced into the system that can undergo fusion per fueling event. If the fuel is in a discrete form, such as an IFE pellet or capsule, η_f is equal to unity. If the fuel is provided by other concepts, such as one in which an initial plasma is formed via tritium fueling, only some of the plasma will participate in the ignition event, and $\eta_\mathrm{f} < 1$ in this case. Because the energy gain per fusion reaction is fixed, f_b and η_f describe exactly the amount of fusion energy released per event, and therefore characterize the energy gain, a key fusion performance metric. The ICF or MIF FPP designer maximizes the $f_\mathrm{b}\eta_\mathrm{f}$ product to maximize gain and fusion energy production, and by definition, also maximizes the effectiveness of tritium consumption. The designer must consider how to recover ash particles and unburned fuel via processes which are outside the timeline of the fusion burn event itself, and which therefore cannot directly impact the fusion performance.

However, this is not the case in equilibrated plasma fusion systems, in which the tritium fueling process, and the fusion itself, is quasi-continuous and not a series of discrete events. Fuel introduction, use, and ash removal are happening concurrently, and therefore interactions between these processes are not decoupled. In this analysis we assume that the fusion plasma has a sufficient duration such that the plasma and surrounding systems are in full equilibrium (for MCF this would typically require pulse duration $>$10–100 s). This time-averaged equilibrium constraint remains even if fueling occurs in discrete events (e.g. pellets, gas puffs) because these, by definition, must occur on timescales shorter than global particle confinement $\sim$1–10 s. Applying this equilibrium requirement we will show that tritium fuel use is directly linked to available fusion performance, and this link is more accurately described by TBE rather than $\eta_\mathrm{f} f_\mathrm{b}$.

The purpose of this work is to derive the expressions needed to calculate TBE, consider the design parameters that govern TBE, and understand the constraints that these parameters will place on fusion performance in burning and commercial magnetic fusion devices. We provide example quantitative assessments of TBE using published data from tokamaks, which have the most mature and extensive results available. However, it should be noted that this analysis is generic to any equilibrated fusion plasma. The script to reproduce the derivations and figures in this paper is available on GitHub [5].

2. Deriving an expression for TBE

2.1. Key definitions

We define the TBE as the fraction of tritium particles entering the principal plasma vacuum vessel (VV) that undergo a D–T fusion reaction:

$$\mathrm{D} + \mathrm{T} \rightarrow \alpha\ (3.5\,\mathrm{MeV}) + \mathrm{n}\ (14.1\,\mathrm{MeV}). \tag{1}$$

An illustration of the key processes and parameters involved in TBE is shown in figure 1. $\dot{N}_\mathrm{T,in}$ is defined as the rate at which neutral tritium particles enter the VV, with units of tritium atoms per second. $\dot{N}_\mathrm{T,burn}$ describes the rate at which tritium is burned through D-T reactions. Every D–T fusion reaction produces a 3.5 MeV alpha (α) particle, i.e. a bare helium (He) nucleus, commonly referred to as helium ash. This fusion byproduct is produced in the core plasma at a rate of $\dot{N}_\alpha$ ash particles per second. For clarity we use α to denote helium ash nuclei in the high temperature core only (helium exhausted in the divertor is referred to as 'He'). We define the 'Tritium Burn Efficiency' TBE as the fraction of tritium particles introduced into the VV that undergo a D–T fusion reaction. Key points to the derivation are:

- The VV represents the boundary within which we define TBE. The VV is the region into which neutral particles enter and leave.
- Neutral particles (D, T) may enter the VV via multiple delivery technologies (e.g. gas, pellets, or plasmoids). Neutral particles (D, T, He) leave the VV via pumping action on the VV. Pumping is the only significant exit pathway for fuel and ash particles. For simplicity we will not directly consider inventory build-up of fuel and ash species in internal VV components. With the exception of plasma-deposited low-Z layers, the in-vessel inventory will saturate.
- Particle entry and exit rates are calculated assuming that the plasma, fusion power and neutral species are in full equilibrium.

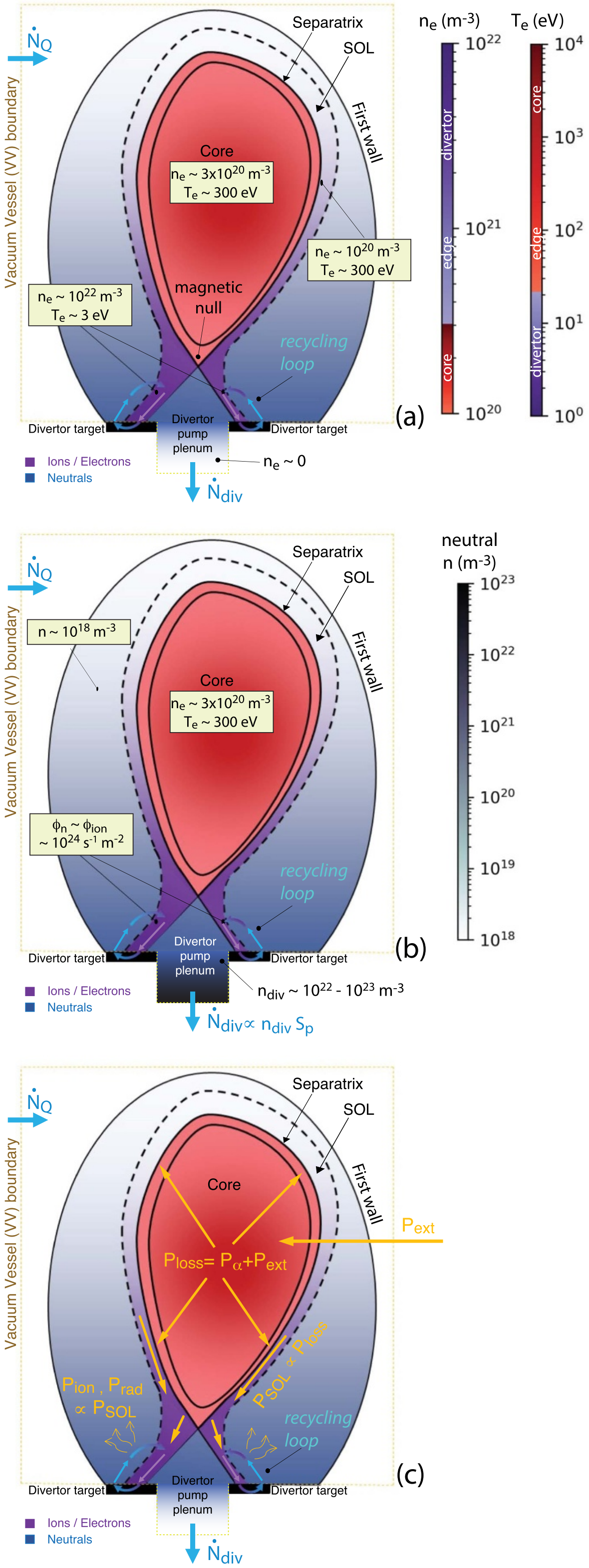

Figure 1. Illustration of key processes and parameters in a equilibrated magnetic fusion device using a dissipative divertor (*a*) plasma density and temperature (*b*) neutrals (*c*) power.

- Particles (e.g. unburned fuel and helium ash exiting the divertor) are neutral unless otherwise specified.
- The D:T ratio is set at 1:1 to maximize fusion reactivity.
- We consider only the fuel and He ash particles. Implications for other non-fusing impurity species will be discussed in later sections.
- High fusion gain requires that helium ash particles from the D–T fusion reaction be well-confined and heat the background plasma through Coulomb collisions. Thus, we assume that the core plasma is designed to force α particles to thermalize into the background plasma on timescales faster than the global energy confinement time ($<$1 s).
- The only significant pathway for the thermalized helium to exit the VV is via pumping at the magnetic divertor(s). The helium is a neutral particle and is exhausted at a rate $\dot{N}_{\mathrm{He,div}}$. The divertors are intentionally designed to produce high neutral gas pressure.

2.2. Derivation

At equilibrium, the burn rate of tritium is equivalent to the production rate of α particles in the core plasma. This is equivalent to the removal rate of helium ash from the divertor, such that helium ash inventory in the divertor is constant:

$$\dot{N}_{\mathrm{T,burn}} = \dot{N}_{\alpha} = \dot{N}_{\mathrm{He,div}}. \tag{2}$$

A constant fuel particle inventory is maintained in the VV. The tritium and deuterium input rate must therefore equal the total exhaust of unburned fuel and He ash from the divertor. Since the D and T ratio is 1:1, we have:

$$\dot{N}_{\mathrm{T,in}} = \dot{N}_{\mathrm{D,in}} = \frac{1}{2}\dot{N}_{\mathrm{Q,in}} \tag{3}$$

and:

$$\dot{N}_{\mathrm{T,div}} = \dot{N}_{\mathrm{D,div}} = \frac{1}{2}\dot{N}_{\mathrm{Q,div}} \tag{4}$$

where Q is used to denote all unburned fuel species atoms regardless of molecular form (DT, D_2, T_2). The VV fuel inventory equilibrium requires that the fueling rate equals the total exhaust rate:

$$\dot{N}_{\mathrm{Q,in}} = \dot{N}_{\mathrm{Q,div}} + 2\dot{N}_{\mathrm{He,div}} \tag{5}$$

where the factor of 2 on the RHS reflects the fact that two Q atoms are required to produce a single He atom. Equivalently one can express the equilibrium condition by:

$$\dot{N}_{\mathrm{T,in}} = \dot{N}_{\mathrm{T,div}} + \dot{N}_{\mathrm{He,div}} = \dot{N}_{\mathrm{D,in}} = \dot{N}_{\mathrm{D,div}} + \dot{N}_{\mathrm{He,div}} \tag{6}$$

which leads to two important definitions of TBE through these equilibrium and equivalence relations:

$$\mathrm{TBE} \equiv \frac{\dot{N}_{\mathrm{T,burn}}}{\dot{N}_{\mathrm{T,in}}} = \frac{\dot{N}_{\alpha}}{\dot{N}_{\mathrm{T,div}} + \dot{N}_{\mathrm{He,div}}} \tag{7}$$

$$\mathrm{TBE} \equiv \frac{\dot{N}_{\mathrm{T,burn}}}{\dot{N}_{\mathrm{T,in}}} = \frac{\dot{N}_{\mathrm{He,div}}}{\dot{N}_{\mathrm{T,div}} + \dot{N}_{\mathrm{He,div}}} = \left(\frac{\dot{N}_{\mathrm{T,div}}}{\dot{N}_{\mathrm{He,div}}} + 1\right)^{-1}. \tag{8}$$

And by using equation (4),

$$\text{TBE} = \left(\frac{\dot{N}_{\text{Q,div}}}{2\dot{N}_{\text{He,div}}} + 1 \right)^{-1}. \tag{9}$$

These definitions of TBE highlight several key points. First, by using these global equilibrium arguments at the VV boundary, we remove the requirement to describe fueling in terms of fueling efficiency η_{f}. Indeed, we do not need to introduce η_{f} to define TBE, which we contend is the more useful and accurate metric in an equilibrated system. Second, through equations (2) and (7), we see that TBE is directly linked to fusion power since $\dot{N}_\alpha$ is equivalent to the fusion reactivity and tritium burn rate. Third, equation (9) shows that TBE is determined by divertor parameters, namely the relative rate of unburned D–T fuel removal to helium ash removal. This arises from the equilibrium concept itself, and is not applicable to fusion FPPs with discrete burn events. When $\dot{N}_{\text{Q,div}}/2\dot{N}_{\text{He,div}}$ decreases, corresponding to a greater rate of He ash removal via pumping, TBE increases. A high TBE—and high fusion power—is dependent on the divertor's ability to efficiently, continuously remove burnt helium ash.

Divertor pumping removal rates are set by the product of the neutral gas density n [# m^{-3}] and effective pumping speed S [m^3 s^{-1}] of each species x:

$$\dot{N}_{\text{x,div}} = n_{\text{x,div}} \cdot S_{\text{x}}. \tag{10}$$

We define the ratio of pumping speeds for helium ash and unburned hydrogenic species that are pumped out of the divertor as:

$$\Sigma \equiv \frac{S_{\text{He}}}{S_{\text{Q}}}. \tag{11}$$

We define the relative density of neutral He ash to hydrogenic fuel in the divertor as:

$$f_{\text{He,div}} \equiv \frac{n_{\text{He,div}}}{n_{\text{Q,div}}}. \tag{12}$$

By substituting equations (10)–(12) into equation (9), we arrive at the following expression:

$$\text{TBE} = \left(\frac{1}{2 f_{\text{He,div}} \Sigma} + 1 \right)^{-1}. \tag{13}$$

Equation (13) provides the important insight that, at fixed pumping speeds, TBE monotonically increases with $f_{\text{He,div}}$. This is shown graphically in figure 2. Yet increasing fractions of He ash has significant consequences to fusion performance, which is the topic of the next section. Imagine that we deployed a theoretical pumping system that enabled $\Sigma \gg 1$. TBE would monotonically increase and asymptote toward unity. This represents an extreme case where only He ash particles are removed from the VV, leaving fuel particles (Q) within the VV boundary until they are burned. Even if such pumping technology becomes available, it is undesirable to operate in such a scenario because it prevents active control

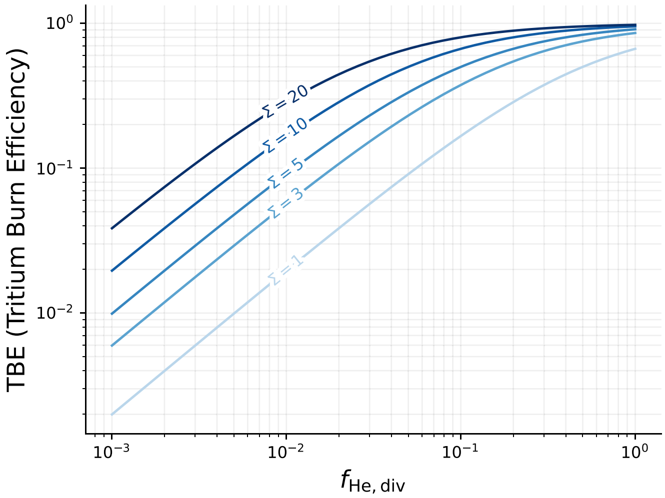

Figure 2. Tritium burn efficiency (TBE) as function of divertor He gas fraction for various values of Σ, the relative effective pumping speed of He and fuel species.

of the fuel plasma density. Nevertheless, equation (13) indicates that there are multiple pathways we can exploit to increase TBE.

3. Divertor function, helium fraction, TBE, and fusion power density

3.1. Divertor function

The primary purpose of a divertor in magnetic fusion device is to create a region inside the VV dedicated to particle exhaust. This is accomplished by creating poloidal magnetic field nulls in the divertor region, which result in open field lines terminating at divertor plates (see figure 1). The nulls define the location of the last closed flux surface and thus determine the volume of the confined plasma where fusion reactions can occur. Due to the extremely large plasma heat conduction ($\kappa_{\|} \propto \text{T}^{5/2}$) and high sonic exit speed ($c_s \propto \text{T}^{1/2} \sim 10^4 - 10^5$ m s^{-1}) that is possible parallel to magnetic field lines [6], the divertor surfaces experience large incident plasma heat flux ($q > 1$ MW m^{-2}) and charged particle flux density ($\Gamma_i \geqslant 10^{23}$ ions s^{-1} m^2). The divertor therefore constitutes the primary location for convective and conductive plasma heat exhaust. The plasma charged particles have small range ($\sim 10^{-9}$ m) in structural materials where they undergo recombination with the incident electrons ($\Gamma_e = \Gamma_i$ is enforced by ambipolarity) that also implant in the surface and neutralize into atoms. Therefore, plasma particle species (D, T, He) reach saturation density ($\sim 10^{28}$ # m^{-3}) in the divertor surfaces at sub-millisecond timescales. The saturated surfaces predominately release volatile neutral gas species back into the local plasma at $\Gamma_{\text{gas}} \simeq \Gamma_i$ via the nearby surface. It is noted that the species under consideration here all form volatile species, with the hydrogenic fuel as diatomic molecules and the helium as atoms. These light (atomic mass M of 1–4) neutral volatiles, near room temperature (RT $\sim$ 0.03 eV) and thus thermal velocities $10^4 \times (\mathrm{T_{RT}/M})^{1/2} \sim 10^3$ m s^{-1} [6], primarily ionize in the plasma near the divertor surface. These neutrals have ionization mean-free-paths $\lambda_{\mathrm{ion}} \sim$ 1–10 mm, which is much smaller than the geometric distance from the divertor surface to the confined core plasma (∼100–500 mm). Therefore, the vast majority of these ionized particles return along magnetic field lines to the nearby divertor surface. This establishes a 'recycling loop' (figure 1) of particle ionization and neutralization with characteristic timescale $\tau_{\mathrm{recycle}} = \lambda_{\mathrm{ion}}/v_{\mathrm{th}} \sim$ 1–10 μs. This is 5–6 orders of magnitude faster than the global energy and particle confinement time ∼1 s. This recycling process therefore strongly increases plasma and neutral gas density near the divertor. The neutral gas density near the divertor surfaces is typically more than 100× larger than it is elsewhere in the VV [6], and the escape of a small fraction of recycling neutral particles into the divertor pump plenum volume allows for particle removal by pumping (figure 1). Poloidal divertors are by far the leading configuration in MCF. They have established sufficient particle exhaust efficiency (e.g [7]) and are featured in the majority, if not all, of MCF burning plasma designs such as ITER [8] and SPARC [9].

By considering divertor functionality, the following important insights regarding tritium burn and TBE are revealed:

1. It is a misconception to characterize TBE as the chance that a given triton has of burning in the confined plasma (TBE) or being exhausted from the divertor as a neutral species (1-TBE) upon a singular journey through the core. Fuel and ash particles can exit and enter the divertor surfaces many hundreds to thousands of times due to the recycling loop before they burn or leave the VV via the pumps. This is self-consistent with (13), which indicates that no knowledge of fueling efficiency is required to calculate TBE.
2. The recycling loop must be primarily sustained by ionization in the divertor, not particles streaming to the divertor from the core plasma. This is because the recycling timescales are 5–6 orders of magnitude shorter than global particle confinement timescales, i.e. the particles in the recycling loop are re-used over and over. The recycling loop is sustained by *power* transport parallel to magnetic field lines in SOL (scrape off layer) into the divertor (figure 1(*c*)). Ionization (and the associated radiation) is inelastic, expending ∼40 eV per ionization, and thus requires an energy input source.
3. Plasma pressure is $\propto nT$ and is conserved along open field lines of the SOL. As a result, the combination of the recycling loop and parallel heat conduction force the divertor plasma to be more dense and less hot than the SOL in proximity to the core plasma (figure 1(*a*)). The two-point model of Stangeby [6] shows that divertor plasma density, which is proportional to the local gas density, scales non-linearly with the core plasma density ($n_{\mathrm{div}} \propto n^3_{\mathrm{core}}$). Thus one expects divertor particle exhaust to be improved (higher $\dot{N}_{\mathrm{Q,div}}$, $\dot{N}_{\mathrm{He,div}}$) at higher n_{core}.
4. Ionization particle balance in the divertor is a driving consideration for the effectiveness of particle removal because it is fundamentally the process that established recycling. The atomic physics that govern this are highly variable and sensitive to divertor plasma conditions of T_e, n_e and the gas species. Helium is generally harder to ionize than hydrogen due to its closed electron shell and high ionization potential. One can therefore reasonably expect helium to have a slower recycling loop. Ratios of hydrogenic and helium densities, and therefore TBE, are not expected to be constant in the divertor. Due to the strong non-linearity in atomic physics rates (e.g. ionization, recombination), and highly variable divertor plasma conditions, direct measurements of $f_{\mathrm{He,div}}$ are required to determine TBE.

3.2. Helium enrichment and dilution

Helium-to-fuel fraction is critical to both TBE and fusion performance, but this fraction can differ between the core and divertor, as do the plasma conditions (figure 1). To describe this difference, we use the term enrichment, which is defined as:

$$\eta_{\mathrm{He}} \equiv \frac{f_{\mathrm{He,div}}}{f_{\alpha,\mathrm{core}}} \tag{14}$$

where $f_{\mathrm{He,div}}$ and $f_{\alpha,\mathrm{core}}$ are the helium-to-fuel fractions in the divertor plasma and the core plasma respectively [7]. In the core plasma, therefore, we have:

$$f_{\alpha,\mathrm{core}} \equiv \frac{n_\alpha}{n_{\mathrm{Q,core}}} \tag{15}$$

equations (14) and (15) are useful because they can be measured experimentally [7, 10].

Charge neutrality requires:

$$n_e = n_{\mathrm{Q,core}} + 2n_\alpha \tag{16}$$

where n_e is the core electron density. Because the Greenwald density operational limit [11] depends on electron density, it is convenient to define ash dilution fraction as:

$$f_{\mathrm{dil}} \equiv \frac{n_\alpha}{n_e}. \tag{17}$$

By substituting equations (16) and (17) into equation (15), we have:

$$f_{\alpha,\mathrm{core}} = \frac{n_\alpha}{n_e - 2n_\alpha} = \frac{f_{\mathrm{dil}}}{1 - 2f_{\mathrm{dil}}}. \tag{18}$$

We can also solve for f_{dil} in terms of $f_{\alpha,\mathrm{core}}$:

$$f_{\mathrm{dil}} = \frac{f_{\alpha,\mathrm{core}}}{1 + 2f_{\alpha,\mathrm{core}}}. \tag{19}$$

Next, consider core fusion power density P_{f} [MW m^{-3}], defined as:

$$P_f = \frac{n^2_{\mathrm{Q,core}}}{4} R(T)_{\mathrm{DT}}\, k_{\mathrm{B}} E_{\mathrm{DT}} \tag{20}$$

where $R(T)_{\mathrm{DT}}\,[\mathrm{m^3\,s^{-1}}]$ is the temperature-dependent D–T rate coefficient, k_{B} is the Boltzmann constant ($1.6\times10^{-19}\,\mathrm{J\,eV^{-1}}$), and E_{DT} is the energy gain from the D–T fusion reaction (17.6 MeV). We use again Q to denote any fuel species so $n_{\mathrm{Q}}=2n_{\mathrm{D}}=2n_{\mathrm{T}}$ assuming equal isotope mixture for maximized reactivity. By combining equations (15), (17), (18) and (20), we obtain:

$$P_{\mathrm{f}}=[1-2f_{\mathrm{dil}}]^2\,\frac{n_e^2}{4}\,R(T)_{\mathrm{DT}}\,k_{\mathrm{B}}E_{\mathrm{DT}}. \tag{21}$$

Ash dilution therefore decreases the fusion power density. The maximum possible value of fusion power density, $P_{\mathrm{f,max}}$, occurs at zero dilution. We can express the ratio of P_{f} to $P_{\mathrm{f,max}}$—referred to here as the fusion power reduction—in terms of the ash dilution fraction alone:

$$\frac{P_{\mathrm{f}}}{P_{\mathrm{f,max}}}=[1-2f_{\mathrm{dil}}]^2. \tag{22}$$

By using (14) and (19), we can express the fusion power reduction in terms of the divertor helium fraction and enrichment:

$$\frac{P_{\mathrm{f}}}{P_{\mathrm{f,max}}}=\left[1-\left(1+\frac{\eta_{\mathrm{He}}}{2f_{\mathrm{He,div}}}\right)^{-1}\right]^2. \tag{23}$$

Having derived both equation (13), which defines TBE in terms of $f_{\mathrm{He,div}}$ and pumping speed ratio Σ, and equation (23), we have now established a quantitative link between TBE, helium gas fraction in the divertor, effective pumping speeds, and fusion power density at fixed core temperature and electron density n_e.

3.3. Experimental observations of He fraction

The relationship between P_{f} and $f_{\mathrm{He,div}}$ is shown in figure 3 for enrichment (η_{He}) ranging from 0.2–2.0. It is informative to look at experimental results to bound expectations for TBE. Enrichment has been measured experimentally in tokamaks using a D–D fuel mixture with helium artificially introduced into the plasma by gas injection or neutral beams in order to mimic alpha production. On DIII-D, when the pumping efficiency was optimized by placing the divertor strikepoint near the pump plenum entrance, and D_2 fueling was done well outside the divertor to enhance particle flow to the divertor, the enrichment of gas-injected helium was found to be $\eta_{\mathrm{He}}\sim$ 0.9–1.1 and $f_{\mathrm{He,div}}\sim0.05$ [7]. These experiments lacked direct helium pumping (thus no insight into pump efficiency) but the $f_{\mathrm{He,div}}$ imply TBE above 0.1 for the default of Σ (figure 2) with a modest 20% decrease in fusion power density compared to the non-diluted case (figure 3). It is of interest to note that the enrichment of heavier, and easier to ionize, noble species (Ne, Ar) were substantially higher than the observed He enrichment, and increased at higher divertor plasma density. This is consistent with the idea that ionization near the divertor plates is key to divertor enrichment. On JT-60U, $\eta_{\mathrm{He}}\sim1$ was found with their W-shaped divertor [12]. On JET [10], $\eta_{\mathrm{He}}\sim$ 0.3–1.0 was observed, with the general trend being that η_{He} decreased for higher core plasma density $n_{\mathrm{e,core}}$. Helium has the highest ionization potential, 24.6 eV, of any neutral element, and the trend observed on JET likely indicates that helium ionization becomes relatively weaker to hydrogenic species (hydrogen has an ionization potential of 13.6 eV) as the divertor T_e falls below ∼10–15 eV at higher electron density (the two-point model predicts divertor $T_e\propto n_{e,core}^2$). These experimentally measured values of η_{He} presently bound the expected values to ∼0.5–1.0, yet it would clearly be advantageous to obtain more data, and simulations, from present magnetic fusion devices on $f_{\mathrm{He,div}}$.

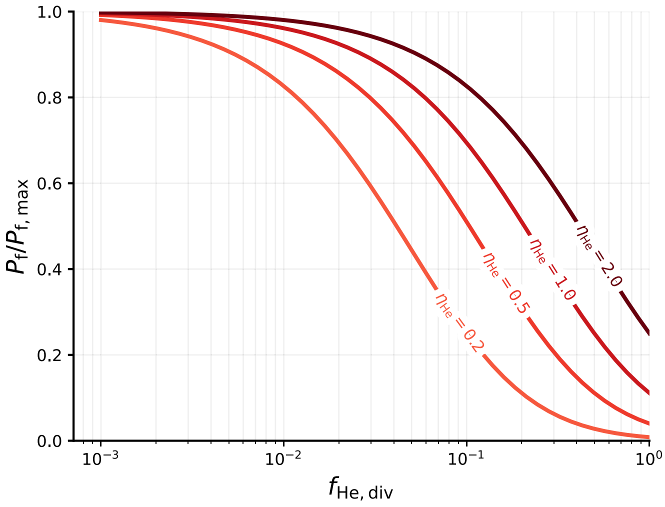

Figure 3. Fusion power density reduction as a function of helium gas fraction in the divertor ($f_{\mathrm{He,div}}$) for values of He divertor enrichment η_{He} ranging from 0.2–2.0, which spans experimental measurements. Higher $f_{\mathrm{He,div}}$ corresponds to greater reduction in P_{f}. Higher divertor enrichment relative to the core corresponds to lower reduction in P_{f}.

3.4. TBE, reduced fusion power density and selective He pumping

At fixed relative pumping efficiency Σ, TBE and $f_{\mathrm{He,div}}$ are monotonically dependent. Moreover, from equations (13) and (23) the fusion power reduction can be expressed as:

$$\frac{P_{\mathrm{f}}}{P_{\mathrm{f,max}}}=\left(1-\frac{1}{\Sigma\eta_{\mathrm{He}}\left(1-\frac{1}{\mathrm{TBE}}\right)}\right)^{-2}. \tag{24}$$

Figure 4 plots P_{f} reduction as a function of TBE for representative values of η_{He} for $\Sigma=1,3,5$, and 10. These plots indicate that achieving high TBE incurs a penalty: it is always accompanied by a reduction in P_{f}, and therefore this is a trade-off that must be considered in the operational design. At $\Sigma=1$ (helium ash and unburned fuel are pumped out of the divertor at equal rates, and there is no attempt to selectively pump out He ash), a reasonable limit for TBE is ∼0.05–0.1. Within the range of η_{He}, ∼ 0.5–1.0, this results in only a 20% reduction in maximum allowed fusion power. When Σ is increased modestly to 3, the TBE at $P_{\mathrm{f}}/P_{\mathrm{f,max}}=0.8$ increases to ∼0.25. At

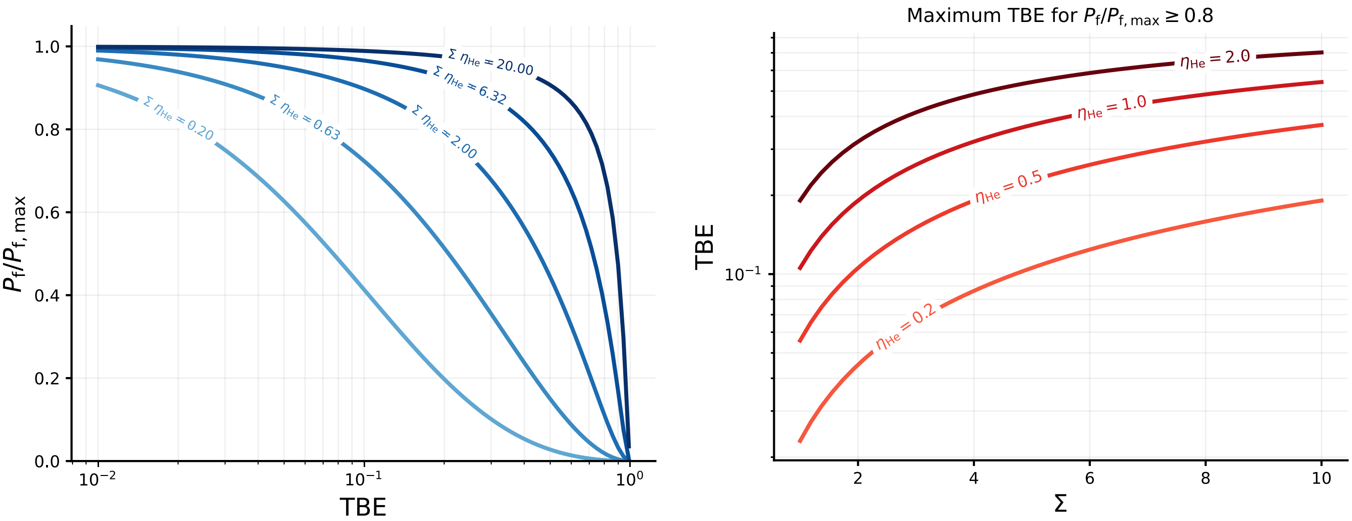

Figure 4. Fusion power density reduction as function of tritium burn efficiency (TBE) for representative values of He divertor enrichment η_{He} and Σ, the relative pumping efficiency of He ash to fuel species (equation (11)). Increasing Σ increases TBE, but high TBE is also correlated to a reduction in fusion power density P_f.

$\Sigma = 10$, TBE reaches even higher values ($\sim$0.5). This exercise informs us that increasing Σ (selectively pumping helium ash out of the divertor at higher rates than unburned fuel particles in the divertor) is a highly effective way to increase TBE to robust levels (TBE $\geqslant 0.1$). Σ can be increased, for example, by designing for selectivity in the gas species that reach the pumping plenum and/or pump surfaces [13], or designing the plant such that some volume of pumped species is filtered for helium ash and then internally recycled [14]. Increasing Σ is flagged as a critical technology development to increase TBE in FPPs.

4. Achieving high TBE and fusion energy gain

The previous section showed that there is a key design tradeoff between high TBE and high P_f, using experimentally determined enrichment parameters to bound the problem. But how do we actually achieve a target TBE and $f_{He,div}$ in a FPP, and how difficult will that be? Furthermore, the minimum allowable value of $P_f/P_{f,max}$ is rather undetermined; is $P_f/P_{f,max} \sim 0.8$ a reasonable compromise?

These questions can be partially answered by further considering power balance and access to fusion gain. Fusion gain Q_p is the ratio of fusion power density P_f to the externally applied heating power density P_{ext}. Reiter *et al* provide a thorough examination of the impact of ash dilution and impurities on access to ignition ($Q_p = \infty$) [15, 16]. We will follow a simplified version of their analysis, ignoring the impact of bremsstrahlung radiation since it plays a minor role for tokamak reactor designs with $T_{core} \geqslant 10$ keV. The effect of other impurities is ignored. Noble elements are often added to enhance radiative power dissipation from the FPP core plasma, thus intentionally introducing another source of fuel dilution. The exact quantity of radiative impurities is highly dependent on the noble species and the core plasma temperature. As shown in [15, 16], these can also close off access to high gain. However, for purposes of generality, we consider here only the He ash effect on dilution.

Power balance in the core requires:

$$P_\alpha + P_{ext} = P_\alpha\,(1 + 5/Q_p) = \frac{W_{th}}{\tau_E} \tag{25}$$

where $\tau_E[s]$ is the energy confinement time, W_{th} [MJ m^{-3}] is the thermal energy density, and P_α is the alpha heating power density, defined as

$$P_\alpha = P_f\,(E_\alpha/E_{DT}) \cong P_f/5 \tag{26}$$

where $E_\alpha = 3.5$ MeV.

With the standard assumption that the species are isothermal, the thermal energy density of the core is expressed as:

$$W_{th} = \frac{3}{2}(n_e + n_{Q,core} + n_\alpha)k_B T = 3n_e k_B T\left(1 - \frac{f_{dil}}{2}\right) \tag{27}$$

where the third term is obtained by applying charge neutrality, per equations (16) and (17).

From equation (21), the full expression for fusion/alpha power density, equations (25) and (27), one obtains:

$$n_e\,\tau_E\,(1 + 5/Q_p) = \left[\frac{12\,T}{E_\alpha R(T)_{DT}}\right]\left[\frac{1 - 0.5 f_{dil}}{(1 - 2f_{dil})^2}\right]. \tag{28}$$

This reverts to the familiar Lawson ignition criterion of $n_e\tau_E \geqslant 1.5 \times 10^{20}$ m^{-3} s for $Q_p = \infty$ and $f_{dil} = 0$, near the broad minimum at $T \sim 25$ keV for the first RHS bracketed term, which depends only on temperature.

As in section 3.2, we can substitute in the relationships between dilution, divertor He fraction, and TBE. Figure 5 shows the $n\tau_E$ performance multiplier that is required on the non-diluted $n\tau_E$ product in order to keep Q_p constant at fixed core temperature. It is difficult to assign a hard limit to the performance multiplier in a design, but >1.5 is unlikely

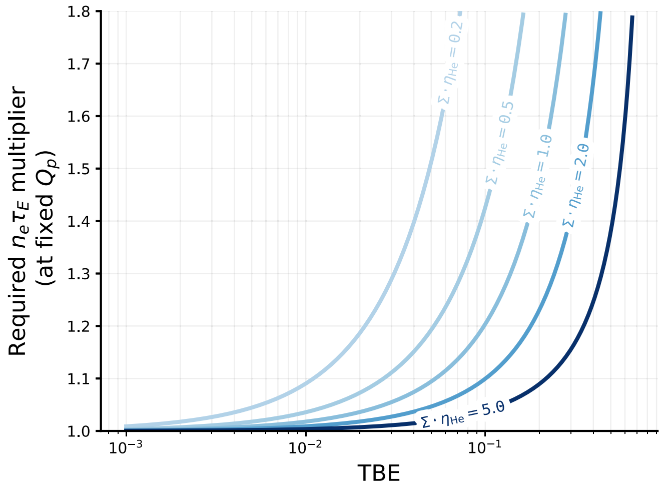

Figure 5. Effect of TBE through dilution on required multiplier to $n\tau_E$ to maintain constant energy gain Q_p (see equation (28)). The curves represent constant values of the product of relative pumping efficiency Σ and He enrichment η_{He}.

to be achieved. This will be due either to proximity to the Greenwald density limit, or to the fact that most fusion plasma designs already seek to maximize confinement, and the statistical spread of empirically predicted confinement values have $+/-15\%$. It is noted that FPP D–T core plasma scenarios often default to the assumption of a few % ash in the core plasma. The primary purpose of figure 5 is to identify the TBE at which the fusion performance multiplier becomes so steep versus TBE that TBE effectively saturates. For example, at $\Sigma \cdot \eta_{He} = 1.0$, this could be estimated to occur at TBE = 0.2, where a 50% increase to TBE = 0.3 requires a doubling in $n\tau_E$.

It is illuminating to consider the effect of dilution and TBE on the ability to achieve a targeted energy gain $Q_{p,0}$ at fixed $n\tau_E$ with no dilution. Figure 6 shows two cases: one where the non-diluted targeted $Q_{p,0} = 10$ (which is typical of burning plasma experimental designs like ITER or SPARC) and the case $Q_{p,0} = 40$ (more typical of power plant designs that must achieve engineering electrical gain $Q_e \geqslant 1$). For the former case, Q_p dropping to 5 or lower is a clear threshold since one drops out of the burning plasma regime where alpha heating dominates. For the latter case, the restrictions on TBE are more severe because the target plasma is highly reliant on alpha heating and this is curtailed by dilution. This further motivates the deployment of technologies that increase Σ in power plant design. TBE will be more important in a power plant and the ability to sustain high Q_p and Q_e will be very sensitive to $\Sigma \cdot \eta_{He}$.

The principal point of these figures and analysis is to show there is an inherent limitation on TBE. This limitation arises because we achieve the target TBE via ash dilution of the divertor plasma, which has implications for the core plasma. If it is possible to design more margin into the core fusion reactivity, for example by having a higher Greenwald fraction/density or more margin in confinement, then TBE can

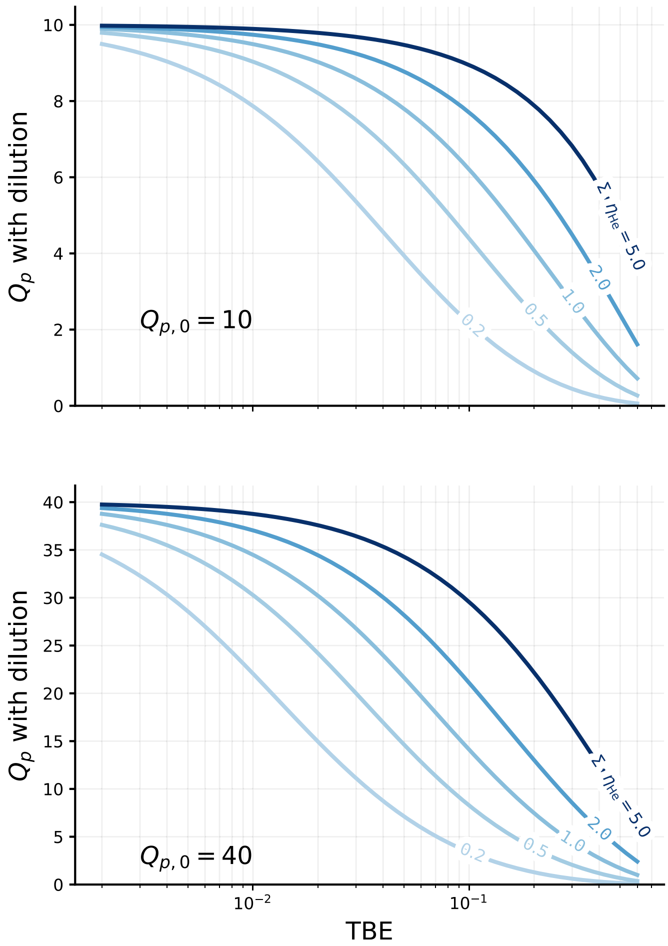

Figure 6. Effect of TBE through dilution on achievable plasma energy gain Q_p. The curves represent constant values of the product of relative pumping efficiency Σ and He enrichment η_{He} (see equation (28)). Two representative curves are provided (top) where non-diluted $Q_{p,0} = 10$ is typical of a burning plasma experiment like ITER or SPARC and (bottom) where $Q_{p,0} = 40$ is typical of a power plant design.

theoretically be increased to higher values. And as previously stated, any increase in Σ via deployment of technology that preferentially increases S_{He} enables the achievement of very high TBE ($\geqslant 0.2$) while maintaining fusion core performance. Fueling efficiency does not play a direct role in setting the limits of TBE. However, it can play a role in accessing the desired operating point of the core plasma. These two criteria—TBE and η_f—should not be confused. This naturally leads to the question of how $f_{He,div}$ and TBE can be 'set' such that that a fusion designer can vary TBE to trade off between efficiencies in the fuel cycle and the overall fusion performance. This has to do with the details of the high-recycling, high gas density divertor region described in section 3 and the design of the associated pumps. For example, the physical proximity of the pumping plenum to regions of high particle density has been found to be important [7].

An interesting example is from JT-60U, which tested various divertor plasma and plenum geometries [12]. These were characterized by measurements of the normalized global helium confinement time τ^*_{He} [s], which is defined by the following relationship:

$$\frac{\tau^*_{\mathrm{He}}}{\tau_{\mathrm{E}}} = \frac{n_\alpha}{\dot{n}_\alpha}\frac{1}{\tau_{\mathrm{E}}} \tag{29}$$

where $n_\alpha[\mathrm{m}^{-3}]$ is the core He density. In the case of JT-60U, the helium was deposited volumetrically into the core plasma using high-energy He neutral beams to mimic α production in the FPP core via fusion reactions. In an FPP, one can define the He/α production rate as:

$$\dot{n}_\alpha = \frac{n_e^2}{4}(1-2f_{\mathrm{dil}})^2\, R(T)_{\mathrm{DT}}. \tag{30}$$

Then, using the previous derivation of equation (28) to rearrange equation (29) into a form that links it directly to dilution and energy gain, one obtains:

$$\frac{\tau^*_{\mathrm{He}}}{\tau_{\mathrm{E}}} = \frac{f_{\mathrm{dil}}}{(1-0.5f_{\mathrm{dil}})}\frac{E_\alpha}{3T}\frac{1}{1+5/Q_{\mathrm{p}}}. \tag{31}$$

Because the target core T is mostly determined by the minimum in the Lawson criterion, $T\sim$ 12–25 keV, the typical term $\frac{E_\alpha}{3T}$ has a value from 50–100. This fact is used to motivate the experimental demonstration of $\tau^*_{\mathrm{He}}/\tau_{\mathrm{E}} \leqslant 10$ such that projected f_{dil} were not excessive for fusion performance at fixed Q_{p}. This is a similar motivation to the assessment of TBE on fusion performance that we have provided here. Importantly, in JT-60U it was found that $\tau^*_{\mathrm{He}}/\tau_{\mathrm{E}}$ could be increased from $\sim$3 up to $\sim$10 by altering the divertor plasma separatrix position. This points to the need to apply modern computational plasma physics tools to better predict the particle pumping efficiency for different FPP configurations.

5. Conclusion

We have formulated TBE, which is a figure of merit describing tritium usage in an equilibrated fusion plasma. TBE defines the rate at which tritium is burned by the fusion plasma compared to the rate of tritium particle injection into the FPP vacuum system. By enforcing equilibrium constraints, the TBE conceptually simplifies the understanding of the controlling parameters, as well as the consequences, for tritium consumption in a FPP. TBE depends on the fraction of He ash particles to unburned fuel particles in the divertor, and the relative pumping speeds at which these species are removed from the system. The TBE concept obviates the need to specify fueling efficiency to characterize tritium usage. Experimental measurements of tokamak divertor helium fraction from 20+ years ago indicate that TBE >5–10% should be achievable. Given the sparse and aged data set, this motivates the need for more experiments on present magnetic fusion devices, including non-tokamak concepts like stellarators, as well as boundary plasma numerical modeling of helium transport and recycling.

The primary consequence of obtaining high TBE is the corresponding increase in the core plasma fuel dilution, which strongly affects fusion power performance. The impact is quantified by the enrichment of the divertor-to-core ash fraction η_{He}. Experimental trends of enrichment vary with operating conditions, but generally indicate that ionization balance, divertor atomic physics, and pump geometry play key roles. Enrichment is also flagged as an important research topic for present day experiments and models. For typical divertor He fractions ($\sim$0.1) and typical enrichment (0.5–1), fusion power density is decreased by 30%–50%. This is a significant penalty to FPP economic performance. When fusion power density is calculated versus TBE, one finds regions of rapid dropoff in power as TBE is increased. The TBE where this dropoff occurs varies significantly. It increases monotonically with the product of enrichment and the ratio of effective pumping speeds Σ. Increased TBE also forces the FPP designer to access higher values of the $n\tau_{\mathrm{E}}$ product to achieve a targeted energy gain Q_{p} values due to dilution. Again, it is found that the required multiplier depends on TBE and the $\eta_{\mathrm{He}}\Sigma$ product. It is further noted that the issue of fusion-product accumulation and removal is a generic issue of concern in all fusion fuel cycles (e.g. D–D, D–^{3}He, p-^{11}B). Some of the charged products have extremely small chances of undergoing fusion (helium,protons) and act as ash, while others (tritium, ^{3}He) may undergo fusion and alter the fusion power balance and the mixture of neutrons. This motivates additional derivations and models for these fuel cycles.

This exercise identifies the need to explore technology solutions such as filtering and direct internal recycling that increase the relative pumping speed at which He ash is removed from the divertor region compared to unburned fuel. The positive news is that rather modest increases to Σ ($\sim$3–5) greatly enhance the permitted TBE (up to $\sim$50%). This indicates that a significant increase in research and development activities devoted to technologies that increase Σ is justified.

ORCID iDs

R. Delaporte-Mathurin https://orcid.org/0000-0003-1064-8882
S.E. Ferry https://orcid.org/0000-0002-7505-9571

References

[1] Abdou M., Riva M., Ying A., Day C., Loarte A., Baylor L., Humrickhouse P., Fuerst T.F. and Cho S. 2020 Physics and technology considerations for the deuterium–tritium fuel cycle and conditions for tritium fuel self sufficiency *Nucl. Fusion* **61** 013001
[2] Clery D. 2022 Out of gas *Science* **376** 1372–6
[3] Wurzel S.E. and Hsu S.C. 2022 Progress toward fusion energy breakeven and gain as measured against the Lawson criterion *Phys. Plasmas* **29** 062103
[4] Kovari M., Coleman M., Cristescu I. and Smith R. 2017 Tritium resources available for fusion reactors *Nucl. Fusion* **58** 026010
[5] Delaporte-Mathurin R. 2023 RemDelaporteMathurin/tritium-burn-fraction: submitted version Zenodo https://doi.org/10.5281/zenodo.8017773

[6] Stangeby P.C. *et al* 2000 *The Plasma Boundary of Magnetic Fusion Devices* (Institute of Physics Publishing) p 224
[7] Wade M. *et al* 1998 Impurity enrichment studies with induced scrape-off layer flow on DIII-D *Nucl. Fusion* **38** 1839
[8] Pitts R., Kukushkin A., Loarte A., Martin A., Merola M., Kessel C., Komarov V. and Shimada M. 2009 Status and physics basis of the ITER divertor *Phys. Scr.* **2009** 014001
[9] Kuang A. *et al* 2020 Divertor heat flux challenge and mitigation in SPARC *J. Plasma Phys.* **86** 865860505
[10] Groth M. *et al* 2002 Helium and neon enrichment studies in the JET Mark IIAP and Mark IIGB divertors *Nucl. Fusion* **42** 591
[11] Greenwald M. 2002 Density limits in toroidal plasmas *Plasma Phys. Control. Fusion* **44** R27
[12] Sakasai A. *et al* 1999 Helium exhaust in ELMy H-mode plasmas with W-shaped pumped divertor of JT-60U *J. Nucl. Mater.* **266** 312–7
[13] Field R., Kuang A.Q., Kim L., Chow C.M., Persad A., Cheng C., Karnik R. and Chiodini A. 2021 Analysis of membrane separation system configurations for the arc fusion reactor *OMC Med Energy Conf. and Exhibition (OnePetro)* (*Ravenna, Italy*, *September 2021*) (available at: https://onepetro.org/OMCONF/proceedings-abstract/OMC21/All-OMC21/473151)
[14] Igitkhanov Y., Day C. and Varoutis S. 2018 A new concept for a higher burn-up fraction improvement in demo reactor *IEEE Trans. Plasma Sci.* **46** 1466–70
[15] Reiter D., Wolf G. and Kever H. 1990 Burn condition, helium particle confinement and exhaust efficiency *Nucl. Fusion* **30** 2141
[16] Reiter D., Kever H., Wolf G., Baelmans M., Behrisch R. and Schneider R. 1991 Helium removal from tokamaks *Plasma Phys. Control. Fusion* **33** 1579